

This is an Open Access document downloaded from ORCA, Cardiff University's institutional repository: <https://orca.cardiff.ac.uk/id/eprint/94852/>

This is the author's version of a work that was submitted to / accepted for publication.

Citation for final published version:

Forootan, E. , Rietbroek, R., Kusche, J., Sharifi, M. A., Awange, J. L., Schmidt, M., Omondi, P. and Famiglietti, J. 2014. Separation of large scale water storage patterns over Iran using GRACE, altimetry and hydrological data. *Remote Sensing of Environment* 140 , pp. 580-595. 10.1016/j.rse.2013.09.025

Publishers page: <http://dx.doi.org/10.1016/j.rse.2013.09.025>

Please note:

Changes made as a result of publishing processes such as copy-editing, formatting and page numbers may not be reflected in this version. For the definitive version of this publication, please refer to the published source. You are advised to consult the publisher's version if you wish to cite this paper.

This version is being made available in accordance with publisher policies. See <http://orca.cf.ac.uk/policies.html> for usage policies. Copyright and moral rights for publications made available in ORCA are retained by the copyright holders.



Separation of large scale water storage patterns over Iran using GRACE, altimetry and hydrological data

Remote Sensing of Environment

Volume 140, January 2014, Pages 580–595

The latest version can be found from

<http://www.sciencedirect.com/science/article/pii/S0034425713003623>

Please Cite

E. Forootan; R. Rietbroek; J. Kusche; M.A. Sharifi; J. Awange; M. Schmidt; P. Omondi; J. Famiglietti (2014). Separation of large scale water storage patterns over Iran using GRACE, altimetry and hydrological data. *Journal of Remote Sensing of Environment*, 140, Pages 580-595, dx.doi.org/10.1016/j.rse.2013.09.025

Separation of large scale water storage patterns over
Iran using GRACE, altimetry and hydrological data,
Journal of Remote Sensing of Environment, 140, Pages
580-595, dx.doi.org/10.1016/j.rse.2013.09.025.

E. Forootan^a, R. Rietbroek^a, J. Kusche^a, M. A. Sharifi^b, J. L. Awange^c, M.
Schmidt^d, P. Omondi^e, J. Famiglietti^f

^a*Institute of Geodesy and Geoinformation (IGG), Bonn University, Bonn, Germany*

^b*Surveying and Geomatics Engineering Department, University of Tehran, Iran*

^c*Western Australian Centre for Geodesy and The Institute for Geoscience Research, Curtin
University, Perth, Australia*

^d*German Geodetic Research Institute (DGFI), Munich, Germany*

^e*IGAD Climate Prediction and Applications Centre (ICPAC), Nairobi, Kenya*

^f*UC Center for Hydrologic Modeling, University of California, Irvine, CA, USA*

Abstract

Extracting large scale water storage (WS) patterns is essential for understanding the hydrological cycle and improving the water resource management of Iran, a country that is facing challenges of limited water resources. The Gravity Recovery and Climate Experiment (GRACE) mission offers a unique possibility of monitoring total water storage (TWS) changes. An accurate estimation of terrestrial and surface WS changes from GRACE-TWS products, however, requires a proper signal separation procedure. To perform this separation, this study proposes a statistical approach that uses a priori spatial patterns of terrestrial and surface WS changes from a hydrological model and altimetry data. The patterns are then adjusted to GRACE-TWS products using a least squares adjustment (LSA) procedure, thereby making the best use of the available data. For the period of October 2002 to March 2011, monthly GRACE-TWS changes were derived over a broad region encompassing Iran. A priori patterns were derived by decomposing the following auxiliary data into statistically independent components: (i) terrestrial WS change outputs of the Global Land Data Assimilation System (GLDAS); (ii) steric-corrected surface WS changes of the Caspian Sea; (iii) that of the Persian and Oman Gulfs; (iv) WS changes of the Aral Sea; and (v) that of small lakes of the selected region. Finally, the patterns of (i) to (v) were adjusted to GRACE-TWS maps so that their contributions were estimated and GRACE-TWS signals separated. After separation, our re-

Email addresses: forootan@geod.uni-bonn.de (E. Forootan), roelof@geod.uni-bonn.de (R. Rietbroek), kusche@geod.uni-bonn.de (J. Kusche), sharifi@ut.ac.ir (M. A. Sharifi), J.Awange@curtin.edu.au (J. L. Awange), M. Schmidt: schmidt@dgfi.badw.de (M. Schmidt), philip.omondi@gmail.com (P. Omondi), jfamigli@uci.edu (J. Famiglietti)

sults indicated that the annual amplitude of WS changes over the Caspian Sea was 152 mm, 101 mm over both the Persian and Oman Gulfs, and 71 mm for the Aral Sea. Since January 2005, terrestrial WS in most parts of Iran, specifically over the center and northwestern parts, exhibited a mass decrease with an average linear rate of ~ 15 mm/yr. The estimated linear trends of groundwater storage for the drought period of 2005 to March 2011, corresponding to the six main basins of Iran: Khazar, Persian and Oman Gulfs, Urmia, Markazi, Hamoon, and Srakhs were -6.7, -6.1, -11.2, -9.1, -3.1, and -4.2 mm/yr, respectively. The estimated results after separation agree fairly well with 256 in-situ piezometric observations.

Keywords: GRACE-TWS, Signal separation, Independent components, Terrestrial and surface water storage, Groundwater, Iran

1. Introduction

Water resource of the Islamic Republic of Iran (Iran) is under pressure due to population growth, urbanization and its related consequences (FAO, 2009). The direct impact of the increasing population (~ 75 million in 2010) on water resources resulted in increased need for fresh water in populated centers, while its indirect impact was an increase in demand of agricultural land and development of irrigation lands (e.g., Ardakani, 2009). Sarraf et al. (2005) state that the total water resources per capita in Iran plunged by more than 65% since 1960, and a decrease of 16% is expected by 2025. The increased demand for groundwater, on one hand, and the high rate of irrigation and over-exploitation of water resources in some areas on the other hand are also likely to become a serious challenge for future protection of groundwater basins of central and northern Iran (Motagh et al., 2008; Mohammadi-Ghaleni and Ebrahimi, 2011).

Since 90% of Iran is located in arid or semi-arid areas, the direct rainfall is its only water recharge. This means that only 10% of the country receives enough rainfall to meet its need while the other much drier parts are heavily dependent on groundwater. Using Synthetic-Aperture Radar (SAR) data, Motagh et al. (2008) showed a land subsidence related to groundwater storage extractions in the central part of Iran between 1971 and 2001. Combining precipitation data with measured piezometric groundwater levels, Van Camp et al. (2012) pointed out that there is an imbalance between exploitation and precipitation recharge in central Iran, which has resulted in the decline of water storage (WS). Their study, however, was restricted to the Shahrekord aquifer (located at $\sim [32.3^{\circ}\text{N}]$ and $[50.9^{\circ}\text{E}]$).

Such conditions, therefore, justify the exploration of alternative monitoring tools that can provide reliable information to improve water policies. These are needed in the management of drought and flood related impacts, as well as improving the overall water situation in the region. Among different hydrological parameters, total water storage (TWS), defined as the summation of all water masses in the Earth's storage compartments (atmosphere, surface waters, ground water, etc.), is an important indicator of the water cycle (Güntner,

32 2008). TWS changes can also be used for evaluating the past and present state
33 of natural resources such as water and fodder, as well as for modeling their
34 future development within the context of human usage and climate change (see
35 e.g., Becker et al., 2010; Grippa et al., 2011; Forootan et al., 2012).

36 For a long time, mapping of terrestrial WS changes mainly relied on piezo-
37 metric observations, in-situ meteorological measurements, as well as hydrolog-
38 ical modeling approaches. Although such approaches are very important for
39 understanding the mechanism of water cycle, they are limited e.g., by data in-
40 consistencies, spatial and temporal data gaps or instrumental and human errors
41 and oversights (Rodell et al., 2007). For Iran, specifically, most of the previ-
42 ous studies focused only on regional water variations, see e.g., Ghandhari and
43 Alavi-Moghaddam (2011). Using such local studies, it is difficult to assess the
44 large scale heterogeneity of the terrestrial water cycle, due to the vast climate
45 and topographic condition of the country (see, e.g., Section 2 and Modarres,
46 2006). Other studies that looked at the large-scale water variations of Iran were
47 restricted to the use of hydrological models (e.g., Abbaspour et al., 2009; Noory
48 et al., 2011).

49 Since March 2002, however, the Gravity Recovery and Climate Experiment
50 (GRACE) is routinely providing satellite-based estimates of changes in TWS
51 within the Earth's system (see e.g., Tapley et al., 2004a,b; Wahr et al., 2004;
52 Kusche et al., 2012; Famiglietti and Rodell, 2013). GRACE-TWS have been
53 used to study regional patterns of TWS changes, e.g., over Asia (e.g., Rodell
54 et al., 2009; Shum et al., 2011; Schnitzer et al., 2013), Africa (e.g., Awange et
55 al., 2013; Becker et al. 2010; Grippa et al., 2011), Australia (e.g., Awange et
56 al., 2011; Van Dijk et al., 2011; Forootan et al., 2012). On a global scale, TWS
57 changes are discussed e.g., in Syed et al. (2008), and Forootan and Kusche
58 (2012). All these studies came to the same conclusion that GRACE-TWS prod-
59 ucts are suitable for studying large scale WS changes on annual and inter-annual
60 time scales.

61 Studies which address TWS changes of the regions around Iran include, for
62 example, the works of Swenson and Wahr (2007) who used satellite altimetry
63 (Jason1) together with GRACE monthly gravity solutions to analyze the WS
64 changes of the Caspian Sea from mid 2002 to 2006, and provided a multi-sensor
65 monitoring of the sea. Avsar and Ustun (2012) showed a downward linear trend
66 of GRACE derived gravity changes over a region including Turkey and west
67 of Iran from 2003 to 2010. Studies of Llovel et al. (2010) and Baur et al.
68 (2013) addressed the basin averaged TWS changes of the Volga River Basin
69 (located in Russia), as well as Tigris-Euphrates region in Iraq. In the same
70 region, Longuevergne et al. (2012) evaluated water variations within the Tigris-
71 Euphrates reservoirs and found a decrease of $\sim 17 \text{ km}^3$ during the drought
72 period between 2007 and 2010. In a recent study, Voss et al. (2013) showed that
73 the pattern of the water loss is extending into the northwestern Iran including
74 the Urmia Basin (see basin 3 in Fig. 1). They also reported that the strong
75 decline of water storage was most likely caused by groundwater depletion in
76 this region between 2003-2009. Our contribution extends these previous studies
77 by looking at the recent patterns of WS changes (from October 2002 to March

78 2011) over the main basins of Iran.

79 Estimating accurate terrestrial or surface WS changes from GRACE-TWS
80 products, however, requires a signal separation approach (e.g., Schmidt et al.,
81 2008; Forootan and Kusche, 2012; Schmeer et al., 2012). This is due to the fact
82 that: (a) GRACE time-variable gravity field products exhibit correlated errors
83 at high degrees (e.g., Swenson and Wahr, 2006; Kusche, 2007; Klees, 2008) that
84 need to be reduced; and (b) GRACE-TWS products represent a mass integral
85 which needs to be separated into their compartments. i.e. the mass varia-
86 tions within Earth’s interior or on its surface or atmosphere. Regarding (a),
87 it is common to apply a filter before computing TWS changes from GRACE
88 time-variable gravity products (e.g., Kusche, 2007). Nevertheless, this filtering
89 introduces biases in the mass change estimations since the mass anomalies are
90 smeared out and moved due to the spatial filtering, known as the ‘leakage’ prob-
91 lem (Swenson and Wahr 2002; Klees, 2007). Fenoglio-Marc et al. (2006; 2012)
92 and Longuevergne et al. (2010) show that the leakage is larger for regions where
93 land meets water reservoirs such as lakes, seas and oceans and also for small
94 basins. To account for these leakages, most of the previous studies focused on
95 basin-wide approaches (e.g., Fenoglio-Marc et al., 2006; 2012; Llovel et al., 2010;
96 Longuevergne et al., 2010; Baur et al., 2013; and Jensen et al., 2013). However,
97 due to the vast size of our region of study, and its varying climatic conditions
98 (see Section 2), it is desirable to implement information extraction methods that
99 allow the retrieval of spatially varying WS changes. This capability is a feature
100 that is usually lost when one applies basin-wide averaging methods.

101 Regarding (b), one may assume that the main source of GRACE-TWS vari-
102 ability consists of the contribution of the terrestrial and surface WS changes
103 (Güntner et al., 2007). We assume that the ocean and atmospheric mass varia-
104 tions have already been removed from GRACE time-variable solutions using
105 de-aliasing products (Flechtner, 2007a,b). Although, this procedure in itself
106 might introduce some errors in TWS estimations (see, e.g., Duan et al., 2012;
107 Forootan et al., 2013), that is not considered in this paper. For partitioning
108 GRACE-TWS, most of the previous studies use altimetry observations to ac-
109 count for the surface WS changes (e.g., Swenson and Wahr, 2007; Becker et al.,
110 2010) and hydrological models for terrestrial water changes (e.g., Syed et al.,
111 2005; Rodell et al., 2007; Van Dijk, 2011; Van Dijk et al., 2011). Subsequently,
112 GRACE-TWS signals are compared or reduced with altimetry and/or model de-
113 rived WS values. The accuracy of the estimation in such approaches might be
114 limited since, for instance, altimetry observations contain relatively large errors
115 over inland waters (e.g. Birkett, 1995; Kouraev et al., 2011) and hydrological
116 models show limited skill (e.g., Grippa et al., 2011; Van Dijk, 2011).

117 In this study, however, instead of removing those surface and terrestrial WS
118 (respectively derived from altimetry and hydrological models) from GRACE-
119 TWS maps, we use them as a priori information, to introduce the spatial pat-
120 terns of surface and terrestrial WS changes. Then GRACE-TWS signals are
121 separated by adjusting the derived spatial patterns to GRACE-TWS maps. For
122 this means, TWS data within a rectangular box (between $[23^{\circ}$ to 48° N] and
123 $[42^{\circ}$ to 63° E]) that includes Iran, is extracted from each monthly GRACE-TWS

124 map. As mentioned before, the main source of TWS variability, within each
125 map, consists of the contribution of the terrestrial and surface WS changes
126 (Güntner et al., 2007). In our case, the surface water variations are mainly
127 caused by water reservoirs within the selected box e.g., the Caspian Sea, Per-
128 sian and Oman Gulfs, Aral Sea as well as other small lakes. Note that the
129 effect of self-gravitational forces, other than those of surface and terrestrial WS
130 changes, might be considerable over the region. A discussion can be found in
131 Appendix B.

132 The higher-order statistical method of independent component analysis (ICA)
133 (Foorootan and Kusche, 2012; 2013) is used to identify statistically independent
134 patterns from (i) monthly WS outputs of the Global Land Data Assimilation
135 System (GLDAS) model (Rodell et al., 2004) over the selected rectangular box;
136 (ii) Surface WS changes derived from altimetry observations of Jason1&2 mis-
137 sions over the Caspian Sea; (iii) sea surface heights (SSH)s in the Persian and
138 Oman Gulfs after removing steric sea level changes; (iv) surface WS changes
139 in the Aral Sea; as well as (v) the other main lakes of the selected box. The
140 derived independent patterns of (i) to (v) were used as known spatial patterns
141 (base-functions) in a least squares adjustment (LSA) procedure, to separate
142 GRACE-TWS maps. This procedure gives the opportunity to make the best
143 use of all available data sets in a LSA framework. A similar argument has been
144 pointed out e.g., in Schmeer et al. (2012), who used experimental orthogonal
145 functions of geophysical models in a LSA model for separating global GRACE
146 integral signals. After separation, besides adjusting the terrestrial WS of (i) to
147 GRACE-TWS, and the estimation of surface WS changes of the region (ii to
148 v), for the first time, our study offers changes of the groundwater within the six
149 main basins of Iran (basins are shown in Fig. 1). Our results are also compared
150 with in-situ piezometric measurements.

151 The remaining part of the paper is organized as follows: in Section 2, we
152 briefly describe the study region. The data used in the study is presented in
153 Section 3. Section 4 outlines the analysis methods, and the results of separation
154 are presented and discussed in Section 5. Finally, Section 6 concludes the paper
155 and provides an outlook. The paper also includes two appendices that pro-
156 vide the results of ICA applied on GLDAS and altimetry derived WS changes
157 (Appendix A), and the effect of self-gravitation on the results (Appendix B).

158 **2. The Study Region**

159 *2.1. Geography*

160 Iran with an area of about 1.7 million km² lies between latitudes [24° to
161 40°N] and longitudes [44° to 64°E] (Fig. 1). The landscape of Iran is dominated
162 by rugged mountain ranges that separate various basins from each other. The
163 largest mountain chain is that of the Zagros, which runs from the northwest of
164 the country southwards to the shores of the Persian Gulf and then continues
165 eastwards along most of the southeastern province. Alborz is the other main

166 mountain chain range that runs from the northwest to the east along the south-
167 ern edge of the Caspian Sea. Over 50% of the area between the two main chains
168 are covered by salty swamps of Dasht-e-Kavir and Dasht-e-Lut.

169 *2.2. Basins and Climate*

170 According to FAO (2009), there are 6 main catchments in Iran (i.e. Fig.
171 1) that include, the Central Plateau in the centre (basin 4; Markazi), the Lake
172 Urmia Basin in the northwest (basin 3), the Persian and Oman Gulf basins in
173 the west and south (basin 2), the Lake Hamoon Basin in the east (basin 5), the
174 Kara-Kum Basin in the northeast (basin 6; Sarakhs) and the Caspian Sea Basin
175 in the north (basin 1; Khazar). All these basins, except the Persian and Oman
176 Gulf Basin, are interior. The Markazi basin, covering over half of the area of the
177 country, has less than one third of the total renewable water resources (FAO,
178 2009). Shapes of the basins, their areas, and the percentage of their renewable
179 water resources are summarized in Fig. 1.

180 The climate of Iran is quite extreme. Its northern edge is categorized as
181 subtropical region (Khazar basin in Fig. 1). Whereas the climate of the other
182 parts, i.e. 90% of the country, ranges from arid to semiarid, with extremely hot
183 summers in central and the southern coastal regions. The main source of the
184 input water in Iran is annual precipitation. The highest annual rainfall of 2275
185 mm has been recorded in Rasht, located near the Caspian Sea. Annual rainfall
186 is less than 50 mm in the deserts (FAO, 2009).

187 *2.3. Main Surface Waters of the Region*

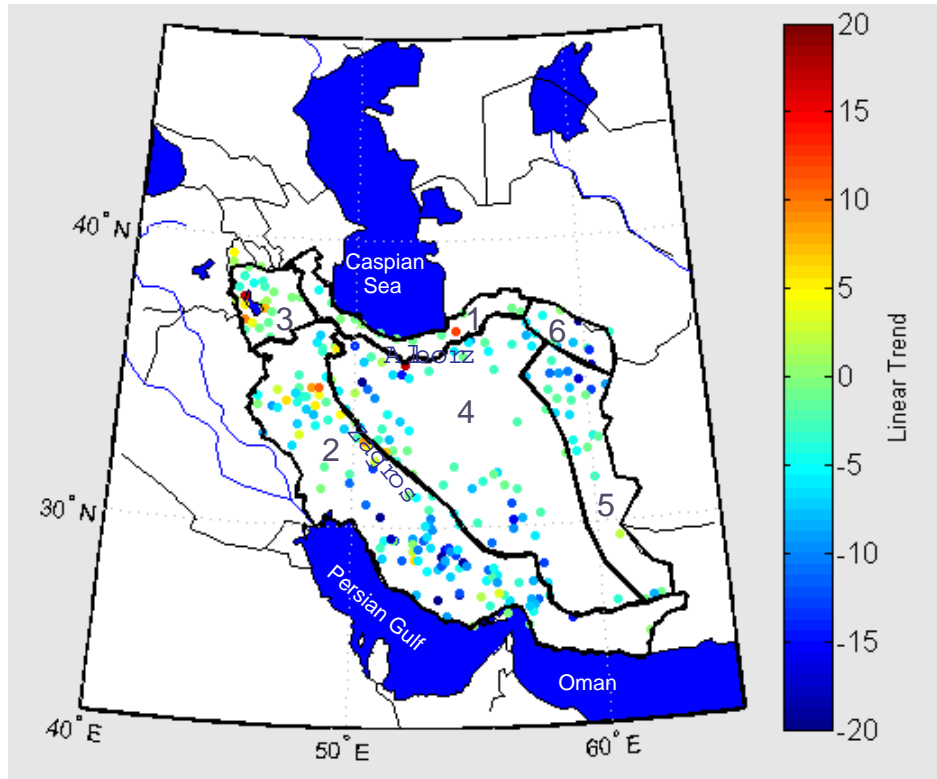
188 *The Caspian Sea*

189 The Caspian Sea, with an area of $\sim 371,000 \text{ km}^2$ is the world's largest inland
190 water body (Kosarev and Yablonskaya, 1994). Kouraev et al. (2011) provide
191 a detailed description on the geographical and physical aspects of the Caspian
192 Sea. The Caspian Sea exhibits considerable fluctuations in its water levels, which
193 have been the subject of several studies (e.g., Kouraev et al., 2011; Sharifi et
194 al., 2013). Using a point-wise technique, Sharifi et al. (2013) illustrated that
195 due to the vast size of Caspian, the varying climatic patterns within the whole
196 sea, and the large impact of the Volga River, each region of the sea is expected
197 to have a water level pattern different from the other regions. Their results
198 indicate that during June 2001 to December 2005 and January 2006 to October
199 2008, linear rates of level variations are respectively 106 and -161 mm/yr. The
200 extreme temperature conditions of the sea also contribute to the changing of
201 the sea level, which exhibits an annual amplitude of $\sim 20 \text{ mm}$ (e.g., Swenson
202 and Wahr, 2007).

203 *Urmia Lake*

204 Lake Urmia (located in the Urmia Basin of Fig. 1, $\sim [37.7^\circ\text{N}$ and $45.31^\circ\text{E}]$) is
205 a salty lake with a surface area of $\sim 5000 \text{ km}^2$ (year 2000). The area of the lake
206 is shrinking, which is partly due to the decade-long drought of its watershed
207 and also due to the construction of 35 dams (since the 1990's) on the rivers

208 which feed the lake. Crétaux et al. (2011) provided altimetry and imagery
 209 results for Lake Urmia (e.g., http://www.legos.obs-mip.fr/en/soa/hydrologie/hydroweb/Page_2.html).
 210



Major Basins of Iran	Percentage of total area of the country	Percentage of total renewable water resources	Number of Stations	Mean of Linear Trend of 2003-2010
1) Khazar	10	15	24	-6 mm/yr
2) Persian and Oman Gulfs	25	46	91	-5 mm/yr
3) Urmia	3	5	19	-13 mm/yr
4) Markazi	52	29	103	-2.5 mm/yr
5) Hamoon	7	2	12	-1.1 mm/yr
6) Sarakhs	3	3	7	-2.3 mm/yr

Figure 1: An overview of in-situ groundwater stations within the six major basins of Iran. The definition of the basins, their areas and renewable water resource percentages are according to FAO (2009). In-situ observations are provided by the Iranian Water-Resource Research Center. The linear rate of water storage change are computed using a least squares approach, while considering the annual and semi-annual frequencies. The Caspian and Aral Sea as well as the Persian and Oman Gulfs are masked out in blue.

211 *The Persian Gulf and the Gulf of Oman*

212 The Persian Gulf, with a surface area of $\sim 251,000 \text{ km}^2$, is a shallow water
213 body in the south (see Fig. 1). Since the Gulf region is surrounded by arid
214 land masses, it has strong seasonal and even daily air temperature fluctuations.
215 Air temperature can drop to 0°C in winter and reach up to 50°C in summer
216 (Kampf and Sadrinasab, 2006), which can contribute to the level fluctuations.
217 Long-term observations of sea level also shows a rise at the head of the Persian
218 Gulf, located in the Tigris-Euphrates delta of southern Iraq and the adjacent
219 regions of southwestern Iran. Lambeck et al. (2002) linked this rise to post
220 glacial rebound.

221 The Gulf of Oman connects the Arabian Sea to the Persian Gulf via the strait
222 of Hormuz. The waters of the Gulf of Oman have more oceanic characteristics
223 than those of the Persian Gulf. However, this does not make the fluctuation of
224 the Gulf greater than the Persian Gulf. Hydrology and circulation aspects of
225 the Oman Gulf are discussed e.g., in Pous et al. (2004).

226 3. Data

227 Four main datasets for the period of 2002 to 2011 were used in this study.
228 These are (a) monthly TWS variations derived from GRACE, (b) surface WS
229 changes derived from satellite altimetry observations, (c) terrestrial WS changes
230 from GLDAS, and (d) 256 in-situ piezometric observations covering the six main
231 basins of Iran. In addition, maps of sea surface temperature (Reynolds et al.,
232 2002) and steric sea level (Ishii and Kimoto, 2009) variations are also used to
233 reduce the contribution of temperature and salinity changes from altimetric
234 SSHs, while converting them to surface WS changes. Note that surface WS is
235 commonly called equivalent water height (EWH) in other studies.

236 3.1. GRACE

237 GRACE, a joint German/USA satellite project, was launched in March 2002
238 to detect mass variations within the Earth's system. In this work, we examined
239 monthly GFZ release 04 gravity field solutions provided by the German Research
240 Centre for Geosciences (GFZ) (Flechtner, 2007b). The data was computed up
241 to degree and order 120 and cover the period from October 2002 to March 2011.
242 GRACE degree 1 coefficients have been augmented by the results of Rietbroek
243 et al. (2009) in order to include the variation of the Earth's center of surface
244 figure with respect to the Earth's centre of mass, in which GRACE products
245 have been computed. We also replaced the zonal degree 2 spherical harmonic
246 coefficients (C_{20}) by values obtained from satellite laser ranging (SLR) (Cheng
247 and Tapley, 2004), which were obtained from the GRACE Tellus Team website
248 (grace.jpl.nasa.gov).

249 GRACE time-variable products contain correlated errors, manifesting itself
250 as a striping pattern (Kusche, 2007). In order to remove the stripes, we applied
251 the de-correlation filter of DDK2 (Kusche et al., 2009) to the GFZ solutions.
252 The choice of the DDK2 filter, which is an anisotropic filter, arises from the

253 consistent results with respect to the outputs of hydrological models (Werth et
254 al., 2009). Before computing monthly TWS fields, residual gravity field solutions
255 with respect to the temporal average over the study period were computed. The
256 residual coefficients were then transformed into $0.5^\circ \times 0.5^\circ$ TWS maps using the
257 approach in Wahr et al. (1998). A rectangular box between ($[23^\circ$ to $48^\circ\text{N}]$ and
258 $[42^\circ$ to $63^\circ\text{E}]$) was then extracted from the monthly TWS grids. For the region
259 of interest, the gridded Root-Mean-Square (RMS) of the GRACE-TWS signals
260 is shown in Fig. 2,A. Strong anomalies are visible over the Caspian Sea, Lake
261 Urmia, as well as over parts of the Zagros and Alborz mountains. The large
262 RMS of the signal over the Caspian Sea and the mountains are due to the strong
263 seasonality of TWS changes. Over Urmia, the strength of the GRACE-derived
264 storage signal is mainly due to the water loss of the lake (see e.g., Voss et al.,
265 2013).

266 3.2. Altimetry Data

267 We used monthly gridded altimetry data over the rectangular region men-
268 tioned above (including the Caspian Sea, the Aral Sea, the Persian and Oman
269 Gulfs, and Urmia Lake as well as other small lakes and reservoirs), cover-
270 ing 2002 to 2011.3. Sea surface heights (SSH)s were originally produced by
271 AVISO and provided through NOAA ERDDAP (the Environmental Research
272 Division’s Data Access Program program, see http://coastwatch.pfeg.noaa.gov/erddap/griddap/noaa_pifsc_9c36_df47_3dd4.html). The RMS of the altimetry
273 signals is shown in Fig. 2,B. For the Caspian Sea, which has the dominant im-
274 pact on the GRACE-TWS signals over the region, we compared NOAA’s SSH
275 with the gridded results of Sharifi et al. (2013), and obtained a correlation of
276 0.91 for the period of 2002 to 2010.

277
278 Water level fluctuations derived from altimetry can be compared to GRACE
279 results, when they are corrected for the so called steric or volumetric height vari-
280 ations caused by temperature and salinity changes (Chambers, 2006). From the
281 areas that contain surface water in this study, the levels of the Caspian Sea
282 and the Persian and Oman Gulfs exhibit a considerable steric component. We
283 used monthly steric sea level changes of Ishii and Kimoto (2009) to convert
284 SSH of the Persian and Oman Gulfs to surface WS changes. Since Ishii and
285 Kimoto (2009)’s study does not cover the Caspian Sea, we followed the ap-
286 proach of Swenson and Wahr (2007) by using SST (sea surface temperature)
287 data and taking a conversion factor of 8.43 mm/yr to convert them to steric
288 sea level changes over the Caspian Sea. The SST data, used here, were recon-
289 structed Reynolds et al. (2002) SST maps obtained from the United States (US)
290 National Oceanic and Atmospheric Administration (NOAA) official website
291 (<http://www.esrl.noaa.gov/psd/data/gridded/data.ncep.oisst.v2.html>). Each
292 map of SSH (after reducing the steric part) was filtered using the same DDK2
293 filter as applied to the GRACE-TWS maps. After applying the DDK2 filter on
294 surface WS data, the mean damping ratio of the filtered data to the original
295 values was ~ 0.71 .

296 *3.3. GLDAS Model*

297 The GLDAS hydrological model integrates a large quantity of observed
 298 data and modeling concepts (Rodell et al., 2004) to produce a global hydro-
 299 logical model. GLDAS terrestrial WS data for the period of study were ob-
 300 tained from the Goddard Earth Sciences Data and Information Services Center
 301 (<http://grace.jpl.nasa.gov/data/gldas/>). Consequently, terrestrial WS consid-
 302 ered here constitutes of total column soil moisture (TSM), Snow Water Equiv-
 303 alent (SWE) and Canopy Water Storage (CWS). Groundwater storage changes
 304 are not represented in the GLDAS model simulations. As a result, our a priori
 305 pattern of the terrestrial storage partitioning is limited, and might not include
 306 a complete description of the lateral and vertical distribution of water storage
 307 up to the surface (see e.g., Rodell and Famiglietti, 2001; Syed et al., 2008). The
 308 GLDAS-WS data were filtered by the same DDK2 filter in order to match the
 309 signal content of the GRACE-TWS fields. The RMS of GLDAS data for the
 310 mentioned rectangular box is shown in Fig. 2,C. The results show strong signals
 311 over the northwest of the country and over the Zagros and Alborz mountains.
 312 The strength of the signal is due to the strong annual variability of TWS over
 313 these regions. We compared the mean magnitude of the DDK2-filtered GLDAS
 314 data with its original values over the region and found a damping ratio of ~ 0.83
 315 due to the filter.

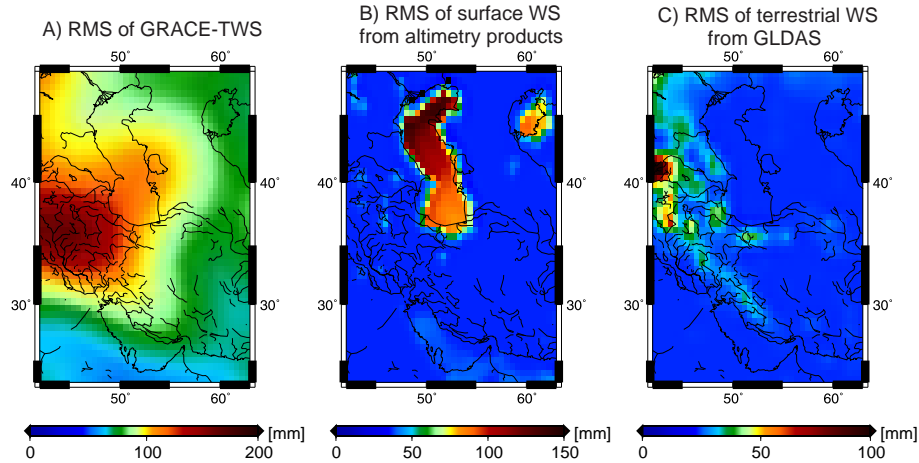


Figure 2: The signal strength (RMS) of the three main data sets used in this study after smoothing using Kusche et al. (2009)’s DDK2 filter; (A) GRACE-TWS data, (B) surface WS from altimetry data and (C) terrestrial WS output of the GLDAS model.

316 *3.4. In-situ Piezometric Measurements*

317 This study used in-situ groundwater observations of 256 selected piezometric
 318 stations of the Iranian Water-resource Research Center, of which 24, 91, 19, 103,
 319 12 and 7 stations are located in the basins one to six of Fig. 1, respectively. The
 320 observations cover the period 2003 to 2010 and have been tested for their quality

321 in terms of outliers and possible biases. The location of the stations and their
 322 computed linear trends for 2003 to 2010 are shown in Fig. 1. In agreement with
 323 the other data, most parts of Iran exhibited a WS decline during the mentioned
 324 period. Note that, there jumps exist in the in-situ time series as a result of
 325 water network changes. Their impact on the computed trends will be addressed
 326 in Section 5.2.

327 4. Methodology

328 Monthly GRACE-TWS maps, used in this study (ocean and atmospheric
 329 mass variations are already removed), reflect an integral measure of the com-
 330 bined effect of terrestrial WS changes of land hydrology (H), and surface WS
 331 changes of seas, lakes and reservoirs (R). Assuming that GRACE-TWS fields
 332 are stored in a matrix $\mathbf{T} = \mathbf{T}(s, t)$, where t is the time, and s stands for spa-
 333 tial coordinate (grid points). \mathbf{T} can be factorized into spatial and temporal
 334 components (Schmeer et al., 2012) as

$$\mathbf{T} = \mathbf{C}_H \mathbf{A}_H^T + \mathbf{C}_R \mathbf{A}_R^T, \quad (1)$$

335 where $\mathbf{C}_{H/R} = \mathbf{C}_{H/R}(t)$ and $\mathbf{A}_{H/R} = \mathbf{A}_{H/R}(s)$ are respectively the temporal
 336 and spatial patterns (base-functions). We used H and R as subindices to show
 337 the base-functions that are computed from terrestrial WS (H) and surface WS
 338 (R). In Eq. 1, \mathbf{C}_H contains zero over the gridpoints of surface water and \mathbf{C}_R
 339 contains zeros over the land.

340 In Eq. 1, once either of $\mathbf{C}_{H/R}(t)$ or $\mathbf{A}_{H/R}(s)$ is determined, the other com-
 341 ponent can be computed by solving a LSA. Schmeer et al. (2012) used a similar
 342 approach for separating global GRACE-TWS integral into its atmospheric, hy-
 343 drologic and oceanic contributors. Their study suggests the application of a
 344 statistical decomposition method on the data/model of each compartment to
 345 compute the required base-functions of Eq. 1. Accordingly, we follow their
 346 approach and use steric corrected SSHs and the WS output from the GLDAS
 347 model as described in Section 3 to compute the required $\mathbf{C}_{H/R}$ and $\mathbf{A}_{H/R}$.

348 ICA, an extension of the second-order statistical method of principal compo-
 349 nent analysis (PCA) (Preisendorfer, 1988), allows the extraction of statistically
 350 independent patterns from spatio-temporal data sets (Cardoso and Souloumiac,
 351 1993). Applications of ICA for filtering (Frappart et al., 2010) and decomposi-
 352 tion of GRACE-TWS are discussed e.g., in Forootan and Kusche (2012; 2013)
 353 and Forootan et al. (2012). Of the two alternative ways of applying ICA, in
 354 which either temporally independent components or spatially independent com-
 355 ponents are constructed (Forootan and Kusche, 2012), we used temporal ICA.
 356 The motivation of this selection was based on the intentions of the study, which
 357 focuses on signals which have distinct temporal behaviour (e.g., seasonal and
 358 trend of water changes). The temporal ICA method is simply called ICA in this
 359 paper, and the decomposition of the centered (temporal mean removed) time
 360 series of \mathbf{H} and \mathbf{R} is written as

$$\mathbf{H} = \bar{\mathbf{P}}_H \hat{\mathbf{R}}_H \hat{\mathbf{R}}_H^T \mathbf{E}_H^T = \mathbf{C}_H \mathbf{A}_H^T, \quad (2)$$

361 and

$$\mathbf{R} = \bar{\mathbf{P}}_R \hat{\mathbf{R}}_R \hat{\mathbf{R}}_R^T \mathbf{E}_R^T = \mathbf{C}_R \mathbf{A}_R^T. \quad (3)$$

362 As stated in Forootan and Kusche (2012), $\bar{\mathbf{P}}_{H/R}$ and $\mathbf{E}_{H/R}$ contain orthogonal
 363 components in their columns that are derived by applying PCA on the centered
 364 data sets of \mathbf{H} and \mathbf{R} (Preisendorfer, 1988). In Eqs. 2 and 3, T is a transpose
 365 operator, $\bar{\mathbf{P}}_{H/R}$ is normalized (i.e. $\bar{\mathbf{P}}_{H/R} \bar{\mathbf{P}}_{H/R}^T = \mathbf{I}$), $\hat{\mathbf{R}}_{H/R}$ is an optimum
 366 rotation matrix that rotates the temporal components of $\bar{\mathbf{P}}_{H/R}$ to make them
 367 temporally as mutually independent as possible (Forootan and Kusche, 2012).

368 As a result of the temporal ICA decomposition, $\mathbf{C}_{H/R} = \bar{\mathbf{P}}_{H/R} \hat{\mathbf{R}}_{H/R}$ con-
 369 tains statistically mutually independent temporal components. $\mathbf{A}_{H/R} = \bar{\mathbf{E}}_{H/R} \hat{\mathbf{R}}_{H/R}$
 370 stores their corresponding spatial maps, that are still orthogonal. $\mathbf{A}_{H/R}$, there-
 371 fore, will be used in Eq. 1 as known spatial patterns and a new temporal
 372 expansions of $\hat{\mathbf{C}}_{H/R}$ will be computed using the LSA approach (e.g., Koch,
 373 1988),

$$[\hat{\mathbf{C}}_H \hat{\mathbf{C}}_R]^T = \left[[\mathbf{A}_H \mathbf{A}_R]^T [\mathbf{A}_H \mathbf{A}_R] \right]^{-1} [\mathbf{A}_H \mathbf{A}_R]^T \mathbf{T}^T. \quad (4)$$

374 In Eq. 4, $\hat{\mathbf{C}}_{H/R}$ contains adjusted temporal components over the land and
 375 surface waters and \mathbf{T} contains GRACE-TWS observations. Then, $\hat{\mathbf{C}}_H$ and $\hat{\mathbf{C}}_R$
 376 can be respectively replaced in Eqs. 2 and 3 to reconstruct terrestrial WS
 377 changes over the land and surface WS changes.

378 5. Numerical Results

379 5.1. Comparison of GRACE and altimetry

380 From Fig. 2,A, the strongest variability during 2002-2011 detected by GRACE
 381 is concentrated over Urmia Lake and the Caspian Sea. Before implementing the
 382 separation approach described in Section 4, we first compared the averaged vol-
 383 ume variations of Urmia and the Caspian Sea derived from GRACE with those
 384 of satellite altimetry. For deriving the time series of the Urmia Basin, we took
 385 the boundary of basin (3) in Fig. 1 as our reference. A basin-averaged TWS
 386 was computed for Urmia Lake using a similar approach to that of Swenson and
 387 Wahr (2007), which is the dash-black line in Fig. 3,A. Then, the contribution
 388 of terrestrial WS surrounding Urmia Lake was removed from GRACE-TWS
 389 using GLDAS data, which is shown as the solid-black line in Fig. 3,A. Our re-
 390 sult of surface WS changes from GRACE is comparable, in terms of cycles and
 391 trend, with those of Crétaux et al. (2011) for Lake Urmia (the solid-gray line in
 392 Fig. 3,A), derived from altimetry and imagery products (<http://www.legos.obs->
 393 [mip.fr/soa/hydrologie/hydroweb/](http://www.legos.obs-mip.fr/soa/hydrologie/hydroweb/StationsVirtuelles/SV_Lakes/Urmia.html) StationsVirtuelles/SV_Lakes/Urmia.html).

394 WS change of the Caspian Sea from GRACE products is shown by the solid-
 395 black line in Fig. 3,B. For computing the averaged surface WS changes over the
 396 Caspian Sea, the average value of steric corrected SSHs was multiplied by the
 397 surface area of the sea and is shown by the solid-gray line in Fig. 3,B. The
 398 correlation coefficient between the two curves is 0.81, at 95% confidence level,
 399 indicating a good agreement. However, in some years (e.g., 2004 and 2008), there
 400 are observable differences between the estimated amplitude of the annual WS
 401 signal from GRACE and altimetry. This could be due to the steric correction
 402 or due to the errors in altimetry data itself. Such observed inconsistencies
 403 motivated the introduced approach for separating GRACE-TWS signals.

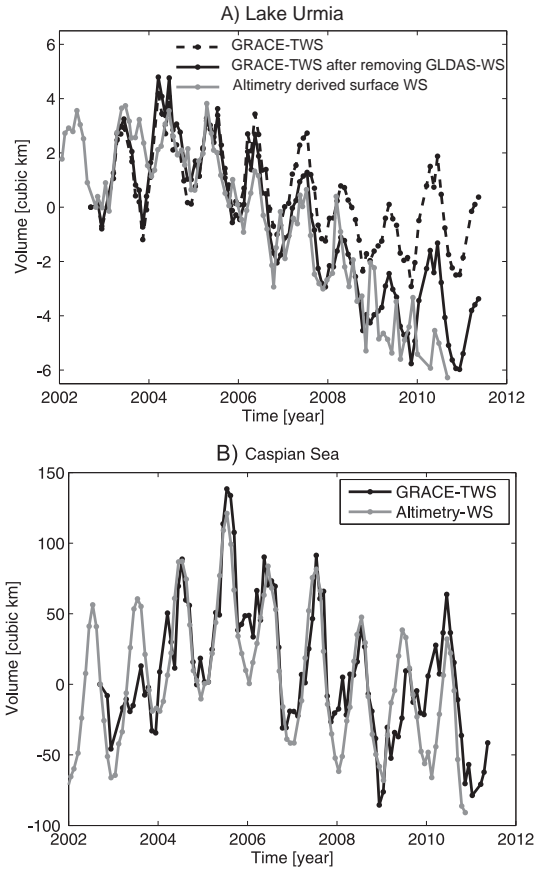


Figure 3: Surface WS changes derived from GRACE and altimetry data, for (A) Lake Urmia and (B) the Caspian Sea. For computing the volume (y-axis), the mean surface area of the Caspian Sea and Urmia Lake (Section 2.3) are multiplied by the mean columns WS changes derived from GRACE and altimetry. During the computations, the shrinking area of Lake Urmia is also taken into account (see also Crétaux et al., 2011).

404 *5.2. Separation (Adjustment) Results*

405 The RMS of GRACE-TWS signals in Fig. 2,A clearly demonstrates the
406 leakage problem. For instance, a part of the Caspian Sea’s WS leaked into its
407 surrounding terrestrial signal or vice versa. In order to separate GRACE-TWS
408 changes, we first extracted independent components of WS changes from altimetry
409 and GLDAS outputs. The results are shown and described in Figs. A1, A2,
410 A3, A4 and A5 of Appendix A. The spatial patterns of the mentioned figures
411 were postulated as known patterns in Eq. 4. We also added four other independent
412 components from GLDAS data to Eq. 4. Note that, in order to restrict the
413 length of the paper, spatial patterns of IC3 to IC6 are not shown in Appendix
414 A. The adjusted temporal patterns of surface and terrestrial WS changes are
415 computed using Eq. 4 and are shown in Figs. 4 and 5, respectively. In this
416 paper, the temporal components are scaled by their standard deviations to be
417 unit-less. Spatial patterns of the figures in Appendix A and B are scaled by the
418 standard deviations of their corresponding temporal components to represent
419 anomaly maps of WS in millimeter.

420 From the annual patterns of surface WS changes, i.e. Fig. 4, A, C, E and
421 F, the amplitude of the adjusted signals are comparable to those of altimetry
422 derived surface WS (EWH) changes. Comparing the adjusted inter-annual
423 changes of surface WS changes (the black lines in Fig. 4,B and D) to their
424 altimetry-derived estimates (the red lines in Fig. 4,B and D) shows that the
425 adjusted values (i.e. coming from GRACE products) are smoother compared
426 to the altimetry results. This is also true for the annual component of the Aral
427 Sea (compare the red and black lines in Fig. 4,E). Investigating the reason for
428 this difference may be the subject of future research.

429 From the adjusted results, we estimate the amplitude of annual surface WS
430 changes of the Caspian Sea to be 150 mm , whereas amplitudes of 101 mm and
431 71 mm are obtained for the Persian and Oman Gulfs, respectively. Fig. 4, E
432 indicates a negative linear trend of $\sim 20\text{ mm/yr}$ during 2002 to 2011 over the
433 Aral Sea.

434 IC1 in Fig. 5,A compares the adjusted value of annual terrestrial WS changes
435 with the WS output of GLDAS. Although, the phase of the signal is comparable,
436 the amplitudes of the signal differ over the years. For instance, an attenuation
437 of the annual amplitudes in the years 2008 and 2009, derived from GRACE
438 (the red line in the temporal pattern of IC1) could be related to the prolonged
439 drought condition over Iran (Shean, 2008). This impact is not fully reflected in
440 the GLDAS outputs (the black line in Fig. 5,A). IC2 of GLDAS (the black line
441 in Fig. 5,B) shows an overall decline of terrestrial WS changes mainly over the
442 central and north-western parts of Iran (see the spatial map of IC2 in Fig. A5).
443 The adjusted value of IC2 (the red line in Fig. 5,B) shows that the drought
444 trend actually starts from 2005. The adjusted results are more consistent with
445 the drought behaviour we found for the small lakes of the country and also in-situ
446 observations, with all showing a decline after 2005. We estimate an average
447 decline of 15 mm/yr water column during 2005 to 2011 over central Iran.

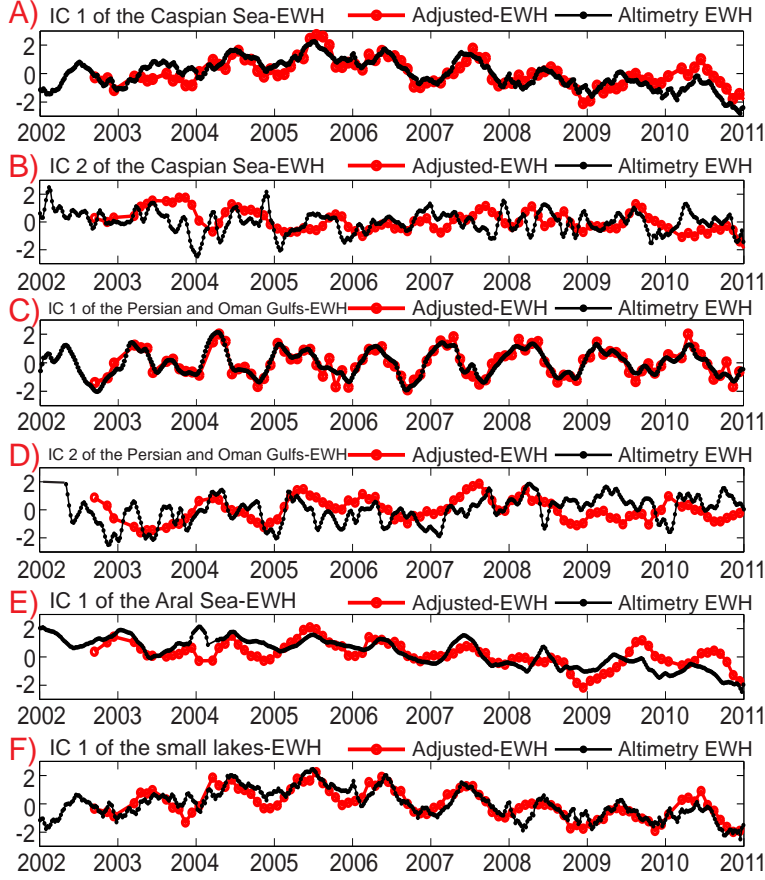


Figure 4: An overview of the adjusted and altimetry derived surface WS changes, shown here in equivalent water height (EWH). The red lines are derived using the LSA method of Section 4 and the black lines are derived from the ICA decomposition of altimetry derived surface WS changes (see Appendix A). (A,B) the first two independent components of the Caspian Sea; (C,D) the first two independent components of the Persian and Oman Gulfs; (E) the first independent component of the Aral Sea; and (F) the first independent component of the small lakes. The temporal patterns are unit-less. The corresponding spatial patterns of (A,B) are shown in Fig. A1; those of (C,D) in Fig. A2; the spatial pattern of (E) in Fig. A3; and that of (F) in Fig. A4. The independent modes are ordered with respect to the variance fraction they represent.

448 *5.3. Comparison of the Adjusted Results with In-situ Observations*

449 Once the signals of the surface and terrestrial WS changes have been sepa-
 450 rated and their amplitudes are adjusted to the GRACE observations, we use the
 451 spatial base-functions derived from GLDAS (i.e. spatial maps of Fig. A5 and
 452 4 other maps that are not shown in the paper) along with their corresponding
 453 adjusted temporal values (the red lines in Fig. 5 and 4 others) in Eq. 2 to re-
 454 construct terrestrial WS changes over Iran. In Eq. 2, the spatial maps stored in
 455 \mathbf{A}_H and \mathbf{C}_H contain the adjusted temporal components. The RMS and linear

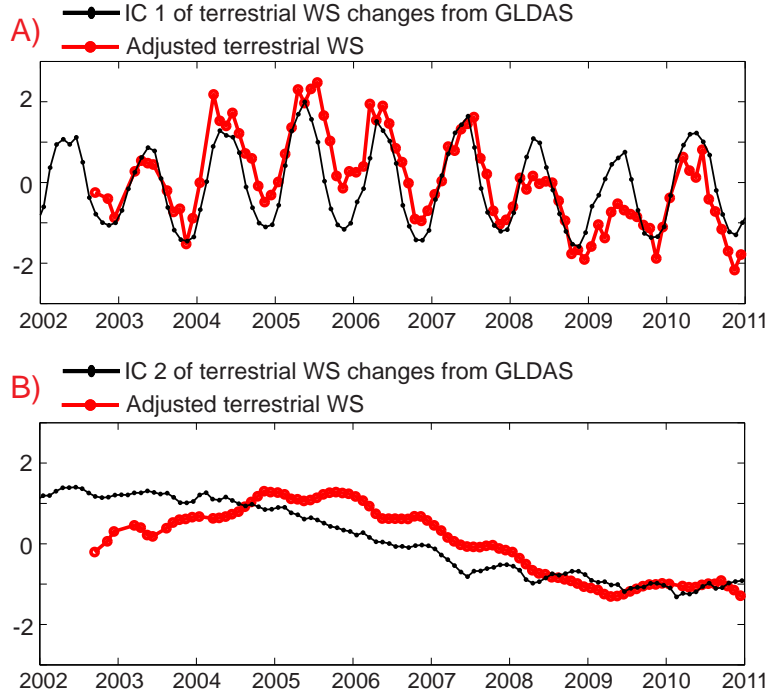


Figure 5: An overview of the main temporal variations of terrestrial WS changes over Iran. The red lines are derived using the LSA method of Section 4 and the black lines are derived from ICA decomposition of GLDAS terrestrial WS changes. (A) corresponds to the first leading independent component, and (B) to the second independent component. The temporal patterns are unit-less and their corresponding spatial patterns are shown in Fig. A5.

456 trends of the reconstructed signals are shown in Fig. 6,A and B, respectively.
 457 The RMS shows that the separation was successful, where for example, the leak-
 458 age caused by the Caspian Sea signal is removed (compare Fig. 6,A with Fig.
 459 2,A). The linear trends (Fig. 6,B) show a decline in most parts of the country
 460 including the northwest, central, as well as over the Zagros chain.

461 We removed the above reconstructed results from GRACE-TWS maps and
 462 compared the results with available in-situ groundwater observations. Before,
 463 comparison, each month of the available stations was first smoothed using a
 464 Gaussian filter of 400 km radius (Jekeli, 1981). The radius of 400 km was se-
 465 lected to be approximately consistent with the DDK2 filter applied to GRACE-
 466 TWS data. We compared the magnitude of the basin averages of the filtered
 467 in-situ observations with those we derived from the original values (in Fig. 1).
 468 We found a mean damping factor of ~ 0.71 , which shows the impact of the
 469 GRACE-like post processing on the true in-situ signals. A comparison of the
 470 results is shown in Fig. 7. The basin averages derived from both in-situ and
 471 satellite observations are consistent in terms of the seasonal peaks and phases.
 472 The linear rates of the water storage changes are depicted in Fig. 7 (dash lines).

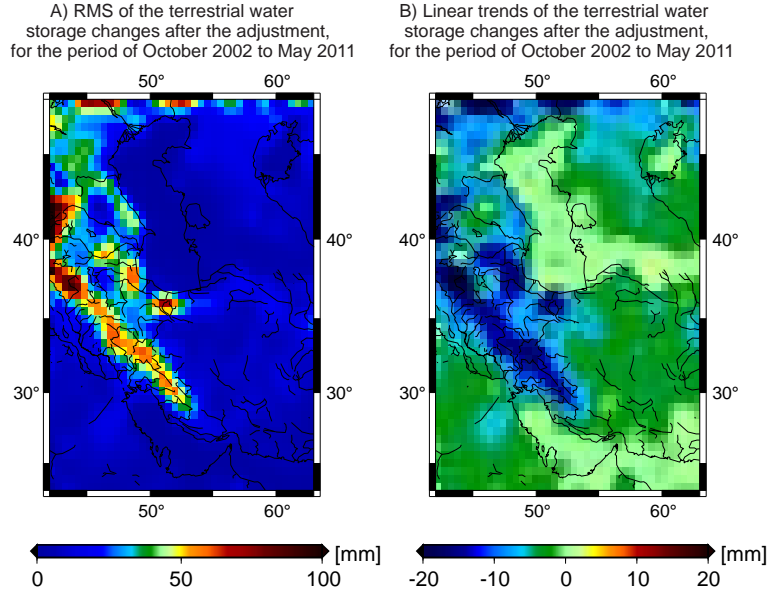


Figure 6: An overview of the reconstructed terrestrial water storage changes over Iran. (A) the RMS of the terrestrial TWS changes after adjusting GRACE-TWS changes (cf. Fig. 2,A) to the base-functions of GLDAS-derived terrestrial WS changes, and (B) the linear trends of the signal in (A).

Basins:	Khazar (Basin 1)	Gulfs (Basin 2)	Urmia (Basin 3)	Markazi (Basin 4)	Hamoon (Basin 5)	Sarakhs (Basin 6)
Groundwater rate of 2003-2005 [mm/yr]:	8.6	5.1	8.5	2.5	1.3	3.7
Groundwater rate of 2005-2011 [mm/yr]:	-6.7	-6.1	-11.2	-9.1	-3.1	-4.2

Table 1: Basin average trends of groundwater variations over the six main basins of Iran derived from GRACE products.

473 As the figure illustrates, in most of the basins, GRACE derived basin averages
 474 tend to show steeper slopes compared to the in-situ observations. Part of this
 475 inconsistency might be the result of network changes in a number of stations.
 476 We removed those stations from our basin average computations and the new
 477 results turned out to be more consistent with that of GRACE (solid gray lines).
 478 The other part of inconsistency might be due to our limited knowledge about
 479 the porosity parameters used for converting piezometer observations to storage
 480 values, which can be quite large for some basins (see e.g., Jiménez-Martínez et
 481 al., 2013). Further research, e.g., involving permanent GPS stations, needs to
 482 be undertaken to address the problem over the selected region. The results of
 483 GRACE-derived groundwater rates are summarized in Table 1.

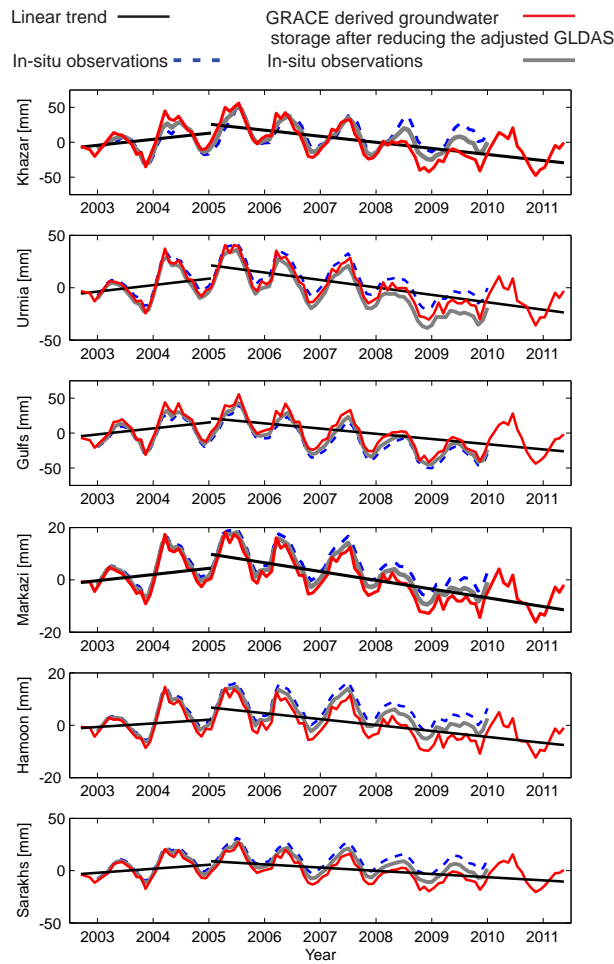


Figure 7: Basin averages of groundwater changes over the six major basins of Iran. The red lines are basin averages after removing the adjusted terrestrial and surface WS changes from GRACE-TWS. The blue dashed lines are derived from in-situ piezometric observations that are located in each basins, respectively. Solid gray lines are derived from the stations, that do not exhibit network changes. Linear trends are shown by the black lines and their rates are reported in Table 1.

484 6. Conclusion and Outlooks

485 The water resources in Iran as a part of the Middle-East region are inherently
 486 scarce as a result of naturally arid climatic conditions. Population increase and
 487 economic growth have spurred higher demands for the limited water resources
 488 (FAO, 2009). Therefore, it is desirable to develop monitoring and analysis tools
 489 to aid understanding the hydrological cycle of the region. In this context, this
 490 study investigated large scale GRACE-TWS pattern changes over a rectangular
 491 region that included Iran for the period from October 2002 to March 2011. The
 492 extracted patterns are important since GRACE-TWS changes represent integral
 493 measurements of water in the entire region. Spatio-temporal changes of TWS,
 494 therefore, may be used to study natural and man-made impacts on the regional
 495 climate.

496 In order to deal with the leakage problem of GRACE products and also

497 to separate terrestrial from surface WS changes, a least squares adjustment
498 approach was applied on the ICA-decomposed terrestrial and surface WS varia-
499 tions respectively from GLDAS and altimetry WS outputs. The applied method,
500 only relies on the ICA-derived spatial patterns of the hydrological model and
501 altimetry observations, which remain invariant in the adjustment. In the ad-
502 justment step, the temporal components are estimated from GRACE-TWS data
503 (Section 5.2). Adjusted terrestrial WS over Iran showed an overall declining
504 trend over the country (Fig. 6,B). In Section 5.3, we demonstrated that the es-
505 timated groundwater storages are in a good agreement with in-situ piezometric
506 observations. Furthermore, for the first time, this study offers GRACE-derived
507 basin averaged groundwater changes for the six main basins of Iran (basins are
508 selected according to FAO, 2009). Our estimates of the linear trends of WS
509 changes for the period of 2003 to 2005 and the drought period of 2005 to 2011.3
510 are shown in Table 1. In view of the low availability of renewable water resources
511 in all the basins, in particular, the Markazi and Urmia basins, the results may
512 be an important incentive for the water resource management of Iran. Note
513 that the area of some of our processed basins, for instance Urmia and Sarakhs,
514 are relatively small and might not meet the nominal resolution of the GRACE-
515 TWS products. However, the strong WS signal of the basins and the proposed
516 optimal processing method allowed retrieval of water storage variations.

517 At the root of the presented separation procedure lies the ICA-decomposition
518 of the GLDAS and altimetry outputs. Such decompositions contain errors as a
519 result of the short length of observations, as well as the errors of observations
520 themselves. Including those errors in the least squares procedure may poten-
521 tially improve the results but falls outside the scope of the current research. The
522 performed separation approach has the potential to be improved by adding extra
523 information on the patterns of water storage variations over the Mesopotamia
524 region, which covers the Tigris/Euphrates River system, Lake Van etc., (see
525 e.g., Voss et al., 2013). The contribution of such base-functions in the inversion
526 will, however, be marginal and concentrated over the basins located at the west
527 part of the country (i.e. basins 2 and 3). The relationship between WS changes
528 in the six major basins of Iran and climate variability such as decadal rainfall
529 anomalies and large scale ocean-atmospheric patterns of e.g., the El Niño South-
530 ern Oscillation phenomenon might be helpful for understanding the water cycle
531 of the region.

532 **Acknowledgement**

533 The authors thank the editor M. Bauer and the anonymous reviewer for
534 the helpful remarks, which improved the manuscript considerably. E. Forootan
535 and J. Kusche are grateful for the financial support provided by the German
536 Research Foundation (DFG) under the project BAYES-G. E. Forootan thanks
537 L. Moxey (the Operations Manager of NOAA OceanWatch - Central Pacific)
538 for the fruitful discussions on altimetry of the Caspian Sea. He also thanks L.
539 Longuevergne (Université de Rennes1) for his useful comments on the performed
540 investigations. The authors also thank Y. Hemmati (Iranian Water-resource

541 Research Center) for providing the in-situ observations. We are grateful for the
542 satellite and model data used in this study. This is a TIGeR Publication no.
543 491.

544 Abbaspour, K.C., Faramarzi, M., Seyed Ghasemi, S., & Yang, H. (2009). Assessing the impact of climate
545 change on water resources in Iran. *Water Resources Research*, 45, W10434, doi:10.1029/2008WR007615.

546 Ardakani, R. (2009). Overview of Water Management in Iran. *Proceeding of Regional Center on Urban Water
547 Management*, Tehran, Iran.

548 Avsar, N.B., & Ustun, A. (2012). Analysis of regional time-variable gravity using
549 GRACE's 10-day solutions. FIG Working Week 2012, Knowing to manage the territory,
550 protect the environment, evaluate the cultural heritage, Rome, Italy, 6-10 May 2012,
551 http://www.fig.net/pub/fig2012/papers/ts04b/TS04B_avsar_ustun_5724.pdf. (accessed date: May 2013)

552 Awange, J.L., Fleming, K.M., Kuhn, M., Featherstone, W.E., Heck, B., & Anjasmara, I. (2011). On the
553 suitability of the $4^{\circ} \times 4^{\circ}$ GRACE mascon solutions for remote sensing Australian hydrology. *Remote Sensing
554 of Environment*, 115, 864-875. doi: 10.1016/j.rse.2010.11.014.

555 Awange, J., Forootan, E., Kusche, J., Kiema, J.K.B., Omondi, P., Heck, B., Fleming, K., Ohanya, S., &
556 Gonçalves, R.M. (2013). Understanding the decline of water storage across the Ramsar-lake Naivasha using
557 satellite-based methods. *Advances in Water Resources*, 60, 7-23, doi:10.1016/j.advwatres.2013.07.002.

558 Bari-Abarghouei, H., Asadi-Zarch, M.A., Dastorani, M.T., Kousari, M.R., & Safari-Zarch, M. (2011). The
559 survey of climatic drought trend in Iran. *Stochastic Environmental Research and Risk Assessment*, 25 (6),
560 851-863, doi:10.1007/s00477-011-0491-7.

561 Baur, O., Kuhn, M., & Featherstone, W.E. (2013). Continental mass change from GRACE over 2002-2011 and
562 its impact on sea level. *Journal of Geodesy*, 87 (2), 117-125, doi:10.1007/s00190-012-0583-2.

563 Becker, M., Llovel, W., Cazenave, A., Güntner, A., & Crétaux, J.-F. (2010). Recent hydrological behavior
564 of the East African great lakes region inferred from GRACE, satellite altimetry and rainfall observations.
565 *Comptes Rendus Geoscience*, 342(3), 223-233. <http://dx.doi.org/10.1016/j.crte.2009.12.010>.

566 Birkett, C.M. (1995). The global remote sensing of lakes, wetlands and rivers for hydrological and climate
567 research, in *Geoscience and Remote Sensing Symposium, 1995. IGARSS 95. 'Quantitative Remote Sensing for
568 Science and Applications'*, Vol 3, 1979-1981.

569 Cardoso J.F., & Souloumiac, A. (1993). Blind beamforming for non-Gaussian signals. In: *IEEE proceedings*,
570 362370. doi:10.1.1.8.5684.

571 Chambers, D.P. (2006). Observing seasonal steric sea level variations with GRACE and satellite altimetry. *J
572 Geophys Res*, 111, C03010, doi:10.1029/2005JC002914.

573 Cheng, M., & Tapley, B.D. (2004). Variations in the Earth's oblateness during the past 28 years. *J Geophys
574 Res*, 109, B09402, doi:10.1029/2004JB003028.

575 Crétaux, J-F., Jelinski, W., Calmant, S., Kouraev, A., Vuglinski, V., Bergé Nguyen, M., Gennero, M-C., Nino,
576 F., Abarca Del Rio, F., Cazenave, A., & Maisongrande, P. (2011). SOLS: A lake database to monitor in near
577 real time water level and storage variations from remote sensing data, *Journal of Advanced Space Research*,
578 1497-1507, doi:10.1016/j.asr.2011.01.004.

579 Duan, J., Shum, C.K., Guo, J., & Huang, Z. (2012). Uncovered spurious jumps in the GRACE atmospheric
580 de-aliasing data: potential contamination of GRACE observed mass change. *Geophys. J. Int.*, 191, 83-87,
581 doi:10.1111/j.1365-246X.2012.05640.x.

582 FAO, (2009). *FAO Water Report 34*.

583 Farrell, W. E., & Clark, J. A. (1976). On postglacial sea level. *Geophysical Journal of the Royal Astronomical
584 Society*, 46(3), 647-667.

585 Famiglietti, J.S., Rodell, M. (2013). Water in the balance. *Science* 340 (6138), 1300-1301,
586 doi:10.1126/science.1236460.

587 Fenoglio-Marc, L., Kusche, J., & Becker, M. (2006). Mass variation in the Mediterranean Sea from
588 GRACE and its validation by altimetry, steric and hydrologic fields. *Geophysical Research Letters*, 33(19),
589 doi:10.1029/2006GL026851.

590 Fenoglio-Marc, L., Rietbroek, R., Grayek, S., Becker, M., Kusche, J., & Stanev, E. (2012). Water
591 mass variation in the Mediterranean and Black Sea. *Journal of Geodynamics*, 59-60, 168-182,
592 <http://dx.doi.org/10.1016/j.jog.2012.04.001>.

593 Flechtner, F. (2007a). AOD1B product description document for product releases 01 to 04. Technical Report,
594 Geoforschungszentrum (GFZ), Potsdam.

595 Flechtner, F. (2007b). GFZ Level-2 processing standards document for level-2 product release 0004, GRACE
596 327-743, Rev. 1.0. Technical Report, Geoforschungszentrum, Potsdam.

597 Forootan, E., Awange, J., Kusche, J., Heck, B., & Eicker, A. (2012). Independent patterns of water mass
598 anomalies over Australia from satellite data and models. *Remote Sensing of Environment*, 124, 427-443,
599 doi:10.1016/j.rse.2012.05.023.

- 600 Forootan, E., & Kusche, J. (2013). Separation of deterministic signals, using independent component analysis
601 (ICA). *Stud. Geophys. Geod.*, Vol.57 (1), 17-26, doi: 10.1007/s11200-012-0718-1.
- 602 Forootan, E., & Kusche, J. (2012). Separation of global time-variable gravity signals into maximally indepen-
603 dent components. *Journal of Geodesy*, 86 (7), 477-497, doi:10.1007/s00190-011-0532-5.
- 604 Forootan, E., Didova, O., Kusche, J., & Löcher, A. (2013). Comparisons of atmospheric data and reduction
605 methods for the analysis of satellite gravimetry observations. *JGR-Solid Earth*, doi: 10.1002/jgrb.50160.
- 606 Frappart, F., Ramillien, G., Leblanc, M., Tweed, S.O., Bonnet, M.P., & Maisongrande, P. (2010). An independ-
607 ent component analysis filtering approach for estimating continental hydrology in the GRACE gravity data.
608 *Remote Sens Environ*, 115(1), 187-204. doi:10.1016/j.rse.2010.08.017
- 609 Ghandhari, A., & Alavi-Moghaddam, S.M.R. (2011). Water balance principles: A review of studies on five
610 watersheds in Iran. *Journal of Environmental Science and Technology*, 4 (5), 465-479, ISSN: 1994-7887,
611 doi:10.3923/jest.2011.465.479.
- 612 Grippa, M., Kergoat, L., Frappart, F., Araud, Q., Boone, A., de Rosnay, P., Lemoine, J.-M., Gascoin, S.,
613 Balsamo, G., Ottlé, C., Decharme, B., Saux-Picart, S., & Ramillien, G. (2011). Land water storage variability
614 over West Africa estimated by Gravity Recovery and Climate Experiment (GRACE) and land surface models.
615 *Water Resour. Res.*, 47, W05549, doi:10.1029/2009WR008856.
- 616 Güntner, A., Stuck, J., Werth, S., Döll, P., Verzano, K., & Merz, B. (2007). A global analysis of temporal and
617 spatial variations in continental water storage. *Water Resour. Res.*, 43, W05416, doi:10.1029/2006WR005247.
- 618 Güntner, A. (2008). Improvement of global hydrological models using GRACE data, *Surv. Geophys.*, 29, 375-
619 397.
- 620 Ishii, M., & Kimoto, M. (2009). Reevaluation of historical ocean heat content variations with time-varying
621 XBT and MBT depth bias corrections. *Journal of Oceanography* 65, 287-299.
- 622 Jekeli, C. (1981). Alternative methods to smooth the Earth's gravity field. Technical report rep 327. Depart-
623 ment of Geodesy and Science and Surveying, Ohio State University, Columbus.
- 624 Jensen, L., Rietbroek, R., & Kusche, J. (2013). Land water contribution to sea level from GRACE and Jason-1
625 measurements. *Journal of Geophysical Research-Oceans*, 118 (1), 212226, doi:10.1002/jgrc.20058.
- 626 Jiménez-Martínez, J., Longuevergne, L., Le Borgne, T., Davy, P., Russian, A., & Bour, O. (2013). Temporal
627 and spatial scaling of hydraulic response to recharge in fractured aquifers: Insights from a frequency domain
628 analysis. *WATER RESOURCES RESEARCH*, 49, 1-17, doi:10.1002/wrcr.20260.
- 629 Kampf, J., & Sadrinasab, M. (2006). The circulation of the Persian Gulf: a numerical study. *Ocean Sci.*, 2,
630 27-41. <http://www.ocean-sci.net/2/27/2006/os-2-27-2006.html>.
- 631 Klees, R., Revtova, E.A., Gunter, B.C., Ditmar, P., Oudman, E., Winsemius, H.C. & Savenije, H.H.G. (2008).
632 The design of an optimal filter for monthly GRACE gravity models. *Geophysical Journal International*, 175(2),
633 417-432, doi:10.1111/j.1365-246X.2008.03922.x.
- 634 Klees, R., Zapreeva, E.A., Winsemius, H.C., & Savenije, H.H.G. (2007). The bias in GRACE estimates of
635 continental water storage variations. *Hydrology and Earth System Sciences Discussions*, 11, 1227-1241.
- 636 Koch, K.R. (1988). Parameter estimation and hypothesis testing in linear models. Springer, New York.
637 ISBN:978354065257.
- 638 Kosarev, A.N., & Yablonskaya, E.A., (1994). The Caspian Sea. The Netherlands:SPB Academic Publishing,
639 pp. 260, ISBN-10:9051030886.
- 640 Kouraev, A.V., Crétaux, J.-F., Lebedev, S.A., Kostianoy, A.G., Ginzburg, A.I., Sheremet, N.A., Mamedov,
641 R., Zakharova, E.A., Roblou, L., Lyard, F., Calmant, S., & Berge-Nguyen, M. (2011). Satellite altimetry
642 applications in the Caspian Sea (Chapter 13). In *Coastal Altimetry*, (Eds) S., Kostianoy, A., Cipollini, P., and
643 Benveniste, J. Springer, 331-366. ISBN:978-3-642-12795-3.
- 644 Kusche, J. (2007). Approximate decorrelation and non-isotropic smoothing of time-variable GRACE-type grav-
645 ity field models. *Journal of Geodesy*, 81, 733-749, doi:10.1007/s00190-007-0143-3.
- 646 Kusche, J., Klemann, V., & Bosch, W. (2012). Mass distribution and mass transport in the Earth system.
647 *Journal of Geodynamics*, 59-60, 1-8, <http://dx.doi.org/10.1016/j.jog.2012.03.003>.
- 648 Kusche, J., Schmidt, R., Petrovic, S., & Rietbroek, R. (2009). Decorrelated GRACE time-variable grav-
649 ity solutions by GFZ, and their validation using a hydrological model. *Journal of Geodesy*, 83, 903-913,
650 doi:10.1007/s00190-009-0308-3.
- 651 Lambeck, K., Esat, T.M., & Potter, E.K. (2002). Links between climate and sea levels for the past three million
652 years. *Nature.*, 2002 Sep 12, 419(6903), 199-206.
- 653 Llovel, W., Becker, M., Cazenave, A., Crétaux, J.-F., & Ramillien, G. (2010). Global land water storage
654 change from GRACE over 2002-2009; Inference on sea level. *Comptes Rendus Geoscience*, 342, (3), 179-188,
655 doi:<http://dx.doi.org/10.1016/j.crte.2009.12.004>.
- 656 Longuevergne, L., Scanlon, B.R., & Wilson, C.R. (2010). GRACE Hydrological estimates for small basins: Eval-
657 uating processing approaches on the High Plains Aquifer, USA. *Water Resources Research*, 46 (11), W11517,
658 doi:10.1029/2009WR008564.

- 659 Longuevergne, L., Wilson, C.R., Scanlon, B.R., & Crétaux, J-F. (2012). GRACE water storage estimates for
660 the Middle East and other regions with significant reservoir and lake storage. *Hydrol. Earth Syst. Sci. Discuss.*,
661 9, 11131-11159, doi:10.5194/hessd-9-11131-2012.
- 662 Modarres, R. (2006). Regional precipitation climates of Iran. *Journal of Hydrology (NZ)* 45 (1), 13-27,
663 ISSN:0022-1708.
- 664 Mohammadi-Ghaleni, M., & Ebrahimi, K. (2011). Assessing impact of irrigation and drainage network on
665 surface and groundwater resources - case study: Saveh Plain, Iran. ICID 21'st International Congress on
666 Irrigation and Drainage, 15-23 October 2011, Tehran, Iran.
- 667 Motagh, M., Walter, T. R., Sharifi, M. A., Fielding, E., Schenk, A., Anderssohn, J., & Zschau, J. (2008). Land
668 subsidence in Iran caused by widespread water reservoir overexploitation. *Geophysical Research Letters*, 35,
669 L16403, doi:10.1029/2008GL033814.
- 670 Noory H., van der Zee, S.E.A.T.M., Liaghat, A.-M., Parsinejad, M., & van Dam, J.C. (2011). Dis-
671 tributed agro-hydrological modeling with SWAP to improve water and salt management of the Voshm-
672 gir irrigation and drainage network in Northern Iran. *Agricultural Water Management*, 98, 1062-1070,
673 doi:10.1016/j.agwat.2011.01.013.
- 674 Pous, S.P., Carton, X., & Lazure, P. (2004). Hydrology and circulation in the Strait of Hormuz and the Gulf
675 of Oman, Results from the GOP99 Experiment: 2. Gulf of Oman. *Journal of Geophysical Research*, 109,
676 C12038, doi:10.1029/2003JC002146.
- 677 Preisendorfer, R. (1988). *Principal component analysis in Meteorology and Oceanography*. Elsevier: Amster-
678 dam, 426 pages. ISBN:044430148.
- 679 Ramillien, G., Famiglietti, J.S., & Wahr, J. (2008). Detection of continental hydrology and glaciology signals
680 from GRACE: a review, *Surv. Geophys.*, 29, 361-374, doi:10.1007/s10712-008-9048-9.
- 681 Reynolds, R.W., Rayne, N.A., Smith, T.M., Stokes, D.C., & Wang, W. (2002). An improved in situ and satellite
682 SST analysis for climate. *J. Clim.*, 15 (2002), pp. 1609-1625.
- 683 Rietbroek, R., Brunnabend, S.E., Dahle, C., Kusche, J., Flechtner, F., Schröter, J., & Timmermann, R. (2009).
684 Changes in total ocean mass derived from GRACE, GPS, and ocean modeling with weekly resolution. *J Geophys*
685 *Res.*, 114, C11004, doi:10.1029/2009JC005449.
- 686 Rietbroek, R., Brunnabend, S.E., Kusche, J., & Schröter, J. (2012). Resolving sea level contributions
687 by identifying fingerprints in time-variable gravity and altimetry. *Journal of Geodynamics*, 59, 72-81,
688 <http://dx.doi.org/10.1016/j.jog.2011.06.007>.
- 689 Rodell, M., Chen, J., Kato, H., Famiglietti, J., Nigro, J., & Wilson, C. (2007). Estimating ground water storage
690 changes in the Mississippi River basin (USA) using GRACE. *Hydrogeol. J.* 15 159-166. doi:10.1007/s10040-006-
691 0103-7.
- 692 Rodell, M., & Famiglietti, J.S. (2001). An analysis of terrestrial water storage variations in Illinois with
693 implications for the Gravity Recovery and Climate Experiment (GRACE), *Water Resour. Res.*, 37(5), 1327-
694 1340, doi:10.1029/2000WR900306.
- 695 Rodell, M., Houser, P.R., Jambor, U., Gottschalk, J., Mitchell, K., Meng, K., Arsenault, C.-J., Cosgrove, B.,
696 Radakovich, J., Bosilovich, M., Entin, J.K., Walker, J.P., Lohmann, D., & Toll, D. (2004). The Global Land
697 Data Assimilation System. *Bulletin of the American Meteorological Society*, 85 (3), 381-394.
- 698 Rodell, M., Velicogna, I., & Famiglietti, J.S. (2009). Satellite-based estimates of groundwater depletion in
699 India. *Nature*, 460, 999-1002, doi:10.1038/nature08238.
- 700 Sarraf, M., Owaygen, M., Ruta, G., & Croitoru, L. (2005). *Islamic Republic of Iran: Cost assessment of*
701 *environmental degradation*, Tech. Rep. 32043-IR, World Bank, Washington, D. C.
- 702 Schmeer, M., Schmidt, M., Bosch, W., & Seitz, F. (2012). Separation of mass signals within GRACE monthly
703 gravity field models by means of empirical orthogonal functions. *Journal of Geodynamics*, 59-60, 124-132,
704 doi:10.1016/j.jog.2012.03.001.
- 705 Schmidt, M., Seitz, F., & Shum, C.K. (2008). Regional fourdimensional hydrological mass variations
706 from GRACE, atmospheric flux convergence, and river gauge data, *J. Geophys. Res.*, 113, B10402,
707 doi:10.1029/2008JB005575.
- 708 Schnitzer, S., Seitz, F., Eicker, A., Güntner, A., Wattenbach, M., & Menzel, A. (2013). Estimation of soil loss
709 by water erosion in the Chinese Loess Plateau using universal soil loss equation and GRACE. *Geophys. J. Int.*,
710 doi:10.1093/gji/ggt023.
- 711 Sharifi, M.A., Forootan, E., Nikkhoo, M., Awange, J., & Najafi-Alamdari, M. (2013). A point-wise least
712 squares spectral analysis (LSSA) of the Caspian Sea level fluctuations, using TOPEX/Poseidon and Jason-1
713 observations. *Advances in Space Research*, 51 (5), 858-873, <http://dx.doi.org/10.1016/j.asr.2012.10.001>.
- 714 Shean, M. (2008). IRAN: 2008/09 wheat production declines due to drought.
715 Commodity intelligence report. United States Department of Agriculture (USDA),
716 http://www.pecad.fas.usda.gov/highlights/2008/05/Iran_may2008.html. Access date: 20.02.2013.
- 717 Shum, C.K., Jun-Yi, G., Hossain, F., Duan, J., Alsdorf, D.E., Duan, X-J, Kuo, C-Y., Lee, K., Schmitt, M.,
718 & Wang, L. (2011). Inter-annual Water Storage Changes in Asia from GRACE Data. In R. Lal et al. (eds.),
719 *Climate Change and Food Security in South Asia*, doi:10.1007/978-90-481-9516-9_6.

720 Swenson, S., & Wahr, J. (2002). Methods for inferring regional surface-mass anomalies from Gravity Recovery
721 and Climate Experiment (GRACE) measurements of time-variable gravity. *Journal of Geophysical Research*,
722 107 (B9), ETG 3-1 - 3-13, doi:10.1029/2001JB000576.

723 Swenson, S., & Wahr, J. (2006). Post-processing removal of correlated errors in GRACE data. *Geophys Res*
724 *Let.*, 33, L08402, doi:10.1029/2005GL025285.

725 Swenson, S., & Wahr, J. (2007). Multi-sensor analysis of water storage variations of the Caspian Sea. *Geophys*
726 *Res Lett.*, 34, L16401, doi:10.1029/2007GL030733.

727 Syed, T.H., Famiglietti, J.S., Chen, J., Rodell, M., Seneviratne, S.I., Viterbo, P., & Wilson, C.R. (2005).
728 Total basin discharge for the Amazon and Mississippi River basins from GRACE and a land-atmosphere water
729 balance. *Geophys. Res. Lett.*, 32, L24404, doi:10.1029/2005GL024851.

730 Syed, T.H., Famiglietti, J.S., Rodell, M., Chen, J., & Wilson, C.R. (2008). Analysis of terrestrial water storage
731 changes from GRACE and GLDAS. *Water Resources Research*, 44, W02433, doi:10.1029/2006WR005779.

732 Tapley, B., Bettadpur, S., Ries, J., Thompson, P., & Watkins, M. (2004a). GRACE measurements of mass
733 variability in the Earth system. *Science*, 305, 503-505. <http://dx.doi.org/10.1126/science.1099192>.

734 Tapley, B., Bettadpur, S., Watkins, M., & Reigber, C. (2004b). The gravity recovery and cli-
735 mate experiment: Mission overview and early results. *Geophysical Research Letters*, 31, L09607.
736 <http://dx.doi.org/10.1029/2004GL019920>.

737 Van Camp, M., Radfar, M., Martens, K., & Walraevens, K. (2012). Analysis of the groundwater resource
738 decline in an intramountain aquifer system in Central Iran. *GEOLOGICA BELGICA* (2012) 15/3: 176-180.

739 van Dijk, A.I.J.M. (2011) Model-data fusion: using observations to understand and reduce uncertainty in hy-
740 drological models. 19th International Congress on Modelling and Simulation, Perth, Australia, 12-16 December
741 2011. <http://mssanz.org.au/modsim2011/index.html>

742 van Dijk, A.I.J.M., Renzullo, L.J., & Rodell, M. (2011). Use of Gravity Recovery and Climate Experiment
743 terrestrial water storage retrievals to evaluate model estimates by the Australian water resources assessment
744 system. *Water Resour. Res.*, 47, W11524, doi:10.1029/2011WR010714.

745 Voss, K.A., Famiglietti, J.S., Lo, M-H., de Linage, C., Rodell, M., & Swenson, S.C. (2013). Groundwater
746 depletion in the Middle East from GRACE with implications for transboundary water management in the
747 Tigris-Euphrates-Western Iran region. *Water Resour. Res.*, 49, doi:10.1002/wrcr.20078.

748 Wahr, J., Molenaar, M., & Bryan, F. (1998). Time variability of the Earth's gravity field: Hydrological and
749 oceanic effects and their possible detection using GRACE. *Journal of Geophysical Research* 103 (B12), 30205-
750 30229, doi:10.1029/98JB02844.

751 Wahr, J., Swenson, S., Velicogna, I., & Zlotnicki, V. (2004). Time-variable gravity from GRACE: First results,
752 *Geophysical Research Letters* paper 10.1029/2004GL019779.

753 Werth, S., Güntner, A., Schmidt, R., & Kusche, J. (2009). Evaluation of GRACE filter tools from a hy-
754 drological perspective. *Geophysical Journal International*, 179, 1499-1515, <http://dx.doi.org/10.1111/j.1365-246X.2009.04355.x>.

756 **Appendix A**

757 *Extracting Independent Components from GLDAS and Altimetry WS Changes*

758 ICA is applied on the data sets on each GLDAS and altimetry data sets
759 using Eqs. 2 and 3 (see the details of application in e.g., Forootan and Kusche,
760 2012). For altimetry products, ICA was individually implemented on (i) the
761 Caspian Sea, (ii) the Persian and Oman Gulfs, (iii) the Aral Sea, and finally
762 (iv) the other small lakes. The results are depicted in Figs. A1, A2, A3 and A4.
763 Note that, similar to the main text, all the temporally independent components
764 (ICs) are unit-less and the spatial patterns are given in millimeters.

765 Fig. A1 shows the first two independent modes, accounting for 93% of the
766 surface WS variance in the Caspian Sea. The remaining 7% of the variance
767 are noisy and are not shown here. IC1 shows an annual behaviour along with
768 two linear trends, one from January 2002 to December 2005 with a rate of 108
769 mm/yr and the other from January 2006 to October 2008 with a rate of -152
770 mm/yr . IC2 indicates the main inter-annual variability from which, the spatial
771 pattern of IC2 shows that the northern part of Caspian exhibits stronger inter-
772 annual variations compared to the central and southern parts (see Fig. A1).
773 This can be related to the climatic extremes, which are more pronounced in the
774 northern part of the Caspian sea inducing stronger mass variations (Kouraev et
775 al., 2011; Sharifi et al., 2013).

776 The ICA decomposition of WS changes of the Persian and Oman Gulfs also
777 shows two significant components explaining 89% of the total variance. IC1
778 shows an annual behaviour with a dipole spatial structure over the two gulfs
779 (see Fig. A2, spatial pattern of IC1). IC2 shows a superposition of inter-annual
780 variability and a positive linear trend ($9 mm/yr$) dominant mainly over the
781 head of the Persian Gulf, where Lambeck et al. (2002) reported a rise due to
782 the post glacial rebound.

783 Fig. A3 shows that only one of the independent component of surface WS
784 changes (corresponding to 89% of the total variance) over the Aral Sea is sta-
785 tistically significant. IC1 of Aral shows the shrinking of the sea with an average
786 linear rate of $300 mm/yr$. Results of ICA, applied on surface WS changes of
787 the small lakes and reservoirs, are shown in Fig. A4. While only the first IC
788 corresponding to 93% of total variance was significant, it shows that most of
789 the surface water of Iran, specifically after the year 2005, are losing water. This
790 situation might be related to the long-term drought condition of the country,
791 see e.g. Bari-Abarghouei et al. (2011).

792 For brevity we only present the first two independent components of GLDAS
793 data, explaining 71% of the total variance of terrestrial WS changes in Fig. A5.
794 The temporal pattern of IC1 shows the dominant annual variation, while the
795 spatial pattern of IC1 is mainly concentrated over north and west Iran. The
796 temporal pattern of IC2 shows an overall linear trend (during 2002 to 2010)
797 corresponding to a decrease of WS over the Markazi and Urmia Basins (see
798 Fig. A5, spatial pattern of IC2). The derived trend appears to differ from the
799 observations of WS changes, e.g., over Urmia (Fig. 3,A) and other small lakes
800 (Fig. A4), where the WS decrease starts from 2005.

801 We should mention here, that to reconstruct 90% of the GLDAS data, one
802 needs to select at least the first six independent components of GLDAS. The
803 temporal behaviours of the remaining four independent components of GLDAS
804 were difficult to interpret and are therefore not plotted. These components were,
805 however, still used in the adjustment procedure.

806 **Appendix B**

807 *Self-gravitational Impact*

808 The strong seasonal mass fluctuations in the Caspian Sea will cause a time
809 variable change in the geoid. On very short time scales (typically days), the
810 ocean will adapt itself to this new equipotential surface, similar to the tidal
811 response of the ocean. This implies that the sea level in the Gulfs and the
812 Black Sea are (indirectly) influenced by the variations in the Caspian Sea. This
813 effect is known as the self-consistent sea level response and has already been
814 described in Farrel and Clarke (1976). When unaccounted for, this effect may
815 potentially mix signal between the base-functions discussed in the main text.
816 We, therefore, quantified its magnitude by taking the steric corrected sea level
817 from altimetry and computed the self consistent sea level response according
818 to Rietbroek et al. (2012). Fig. B1 shows the RMS of this effect. The effect
819 is strongest in the Black Sea, since it is located closest to the Caspian Sea.
820 However the magnitude of the effect is very small compared to the hydrological
821 and oceanic signal sought such that it is not expected to influence the results.
822

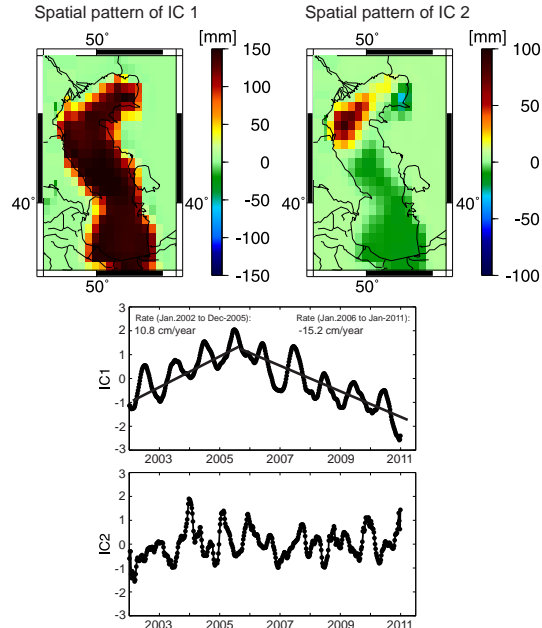


Figure A1: Results of the ICA method applied to the steric corrected SSH data (surface WS changes) over the Caspian Sea. The results are ordered according to their signal strength.

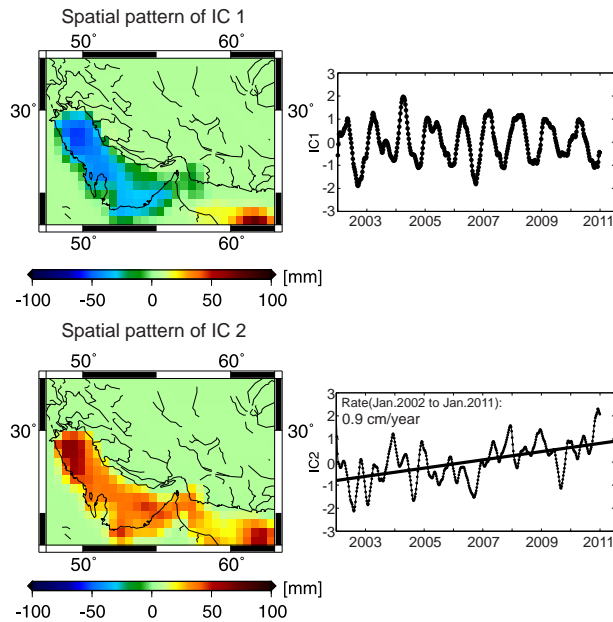


Figure A2: Results of the ICA method applied to the steric corrected SSH data (surface WS changes) over the Persian and Oman Gulfs. The results are ordered according to their signal strength.

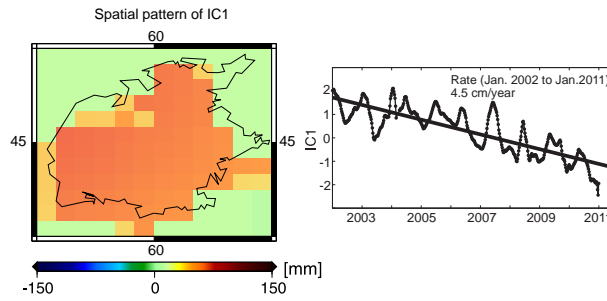


Figure A3: The dominant independent mode of surface WS changes of the Aral Sea.

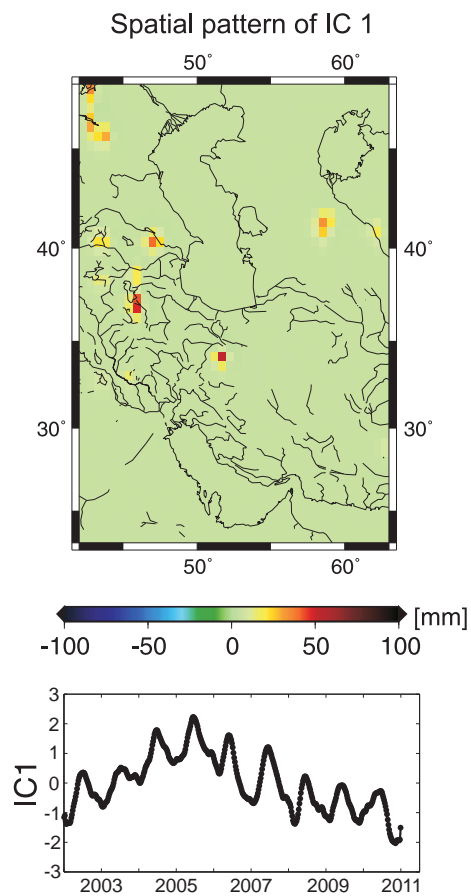


Figure A4: Results of the ICA method applied to the surface WS data over small lakes and reservoirs of the region.

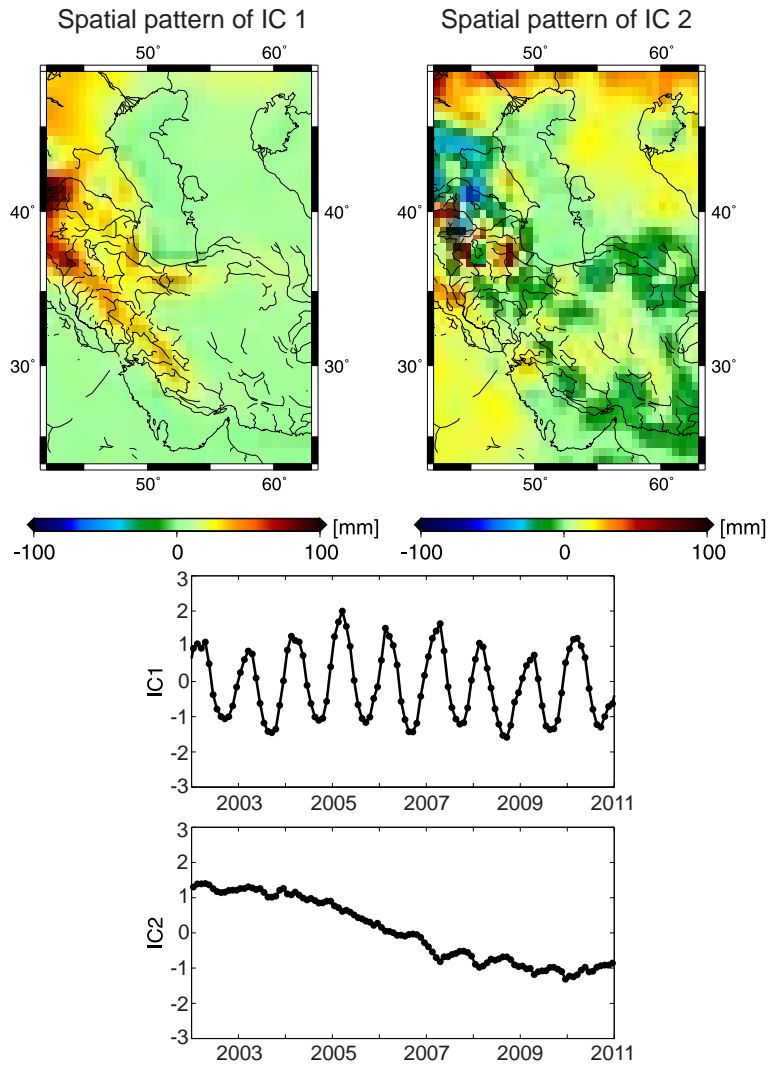


Figure A5: Results of the ICA method applied to the terrestrial WS outputs of the GLDAS model over a rectangular region, including Iran. The components are ordered according to the magnitude of variance they represent.

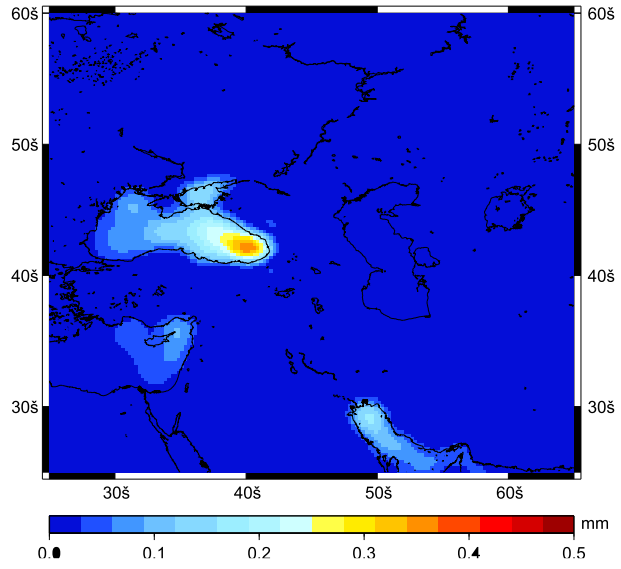


Figure B1: RMS of the self gravitational effect of the Caspian Sea's level variations (steric corrected altimetry) on relative sea level in the Gulfs and the Black Sea.